Metabolic signatures of amyotrophic lateral sclerosis reveal insights into disease pathogenesis

James C. Dodge[a,1], Christopher M. Treleaven[a], Jonathan A. Fidler[a], Thomas J. Tamsett[a], Channa Bao[a], Michelle Searles[a], Tatyana V. Taksir[a], Kuma Misra[a], Richard L. Sidman[b,1], Seng H. Cheng[a], and Lamya S. Shihabuddin[a]

[a]Genzyme, a Sanofi Company, Framingham, MA 01701-9322; and [b]Beth Israel Deaconess Medical Center, Harvard Medical School, Boston, MA 02215

Contributed by Richard L. Sidman, May 11, 2013 (sent for review March 6, 2013)

Metabolic dysfunction is an important modulator of disease course in amyotrophic lateral sclerosis (ALS). We report here that a familial mouse model (transgenic mice over-expressing the G93A mutation of the Cu/Zn superoxide dismutase 1 gene) of ALS enters a progressive state of acidosis that is associated with several metabolic (hormonal) alternations that favor lipolysis. Extensive investigation of the major determinants of H^+ concentration (i.e., the strong ion difference and the strong ion gap) suggests that acidosis is also due in part to the presence of an unknown anion. Consistent with a compensatory response to avert pathological acidosis, ALS mice harbor increased accumulation of glycogen in CNS and visceral tissues. The altered glycogen is associated with fluctuations in lysosomal and neutral α-glucosidase activities. Disease-related changes in glycogen, glucose, and α-glucosidase activity are also found in spinal cord tissue samples of autopsied patients with ALS. Collectively, these data provide insights into the pathogenesis of ALS as well as potential targets for drug development.

carbonic anhydrase | electrolyte | glucagon | glycoproteins | motor neuron disease

Amyotrophic lateral sclerosis (ALS) is a fatal neurodegenerative disorder characterized by the selective loss of motor neurons in the central nervous system (CNS). Approximately 10% of all familial cases of ALS are due to mutations in the gene encoding cytosolic copper–zinc superoxide dismutase (SOD1) (1). Similar to patients with ALS, transgenic mice that express the mutant human SOD1 protein (e.g., $SOD1^{G93A}$ mice) display progressive motor neuron degeneration, muscular atrophy, and a shortened lifespan (2). Although the exact mechanisms and pathological processes responsible for the initiation and progression of motor neuron degeneration remain largely unknown (3), it is becoming increasingly clear that the disorder's basis is multimodal (4).

Acidosis is a feature of several neuropathological conditions including ischemia, epilepsy, Parkinson disease, and multiple sclerosis (5–7). In ALS, an acidic environment has the potential to catalyze the onset and/or progression of several disease features including diminished glutamate reuptake (8), mitochondrial vacuolization (9), glial cell activation (10), endoplasmic reticulum stress (11), and impaired oxidative phosphorylation/ATP synthesis (12). Acidosis also activates acid-sensing ion channels (ASICs), which, when excessively stimulated, promote intracellular Ca^{2+} influx, neuroinflammation, axonal degeneration, demyelination, and neuronal death—features of several mouse disease models (6, 7), including ALS. Interestingly, gene expression profiling studies showed significant up-regulation (2- to 10-fold) of ASIC2 (also known as amiloride-sensitive cation channel neuronal 1; ACCN1) and ASIC3 (ACCN3) in laser-captured motor neurons from patients with ALS harboring mutations in SOD1 (13), suggesting that acidosis occurs in patients with ALS. In agreement, significant up-regulation of ASIC2 expression was recently noted in the spinal cords of patients with sporadic ALS and $SOD1^{G93A}$ mice (14).

Metabolic acid-base disorders are classically identified by measuring the concentrations of plasma or serum electrolytes that affect H^+ concentration. A strong ion difference (SID), the summed ion concentrations of all strong base minus all strong acid, is a major determinant of H^+ concentration. In healthy mammals, SID has a positive value of about 40 mEq/L (15). The apparent SID (SID_{app}), which does not take into account the role of weak acids in determining SID, is calculated as $[Na^+] + [K^+] + [Mg^{2+}] + [Ca^{2+}] - [Cl^-] - [\text{lactate}]$. A more complex Eq. $(1{,}000 \times 2.46 \times 10^{-11} \times pCO_2/(10^{-pH}) + [\text{albumin}] \times (0.12 \times pH - 0.631) + [\text{phosphate}] \times (0.309 \times pH - 0.469)$, the effective SID ($SID_{eff}$), incorporates the contribution of weak acids derived from carbon dioxide (CO_2), proteins (albumin), and phosphate. The difference between SID_{app} and SID_{eff} is called the strong ion gap (SIG), and represents the contribution of unmeasured (i.e., unidentified) ions to the SID. SIG values are reportedly a strong predictor of mortality in individuals exposed to pathological acidosis (16), with the unidentified ions perhaps passing from liver into blood (17). It is not known if disease-related changes in SID_{app}, SID_{eff}, or SIG manifest during development of ALS.

Pathological acidosis can be averted through compensatory mechanisms such as (*i*) lowering acid production (e.g., down-regulating glycogenolysis and glycolysis to inhibit lactate synthesis from glycogen), (*ii*) promoting acid elimination through increased respiration and renal excretion, and (*iii*) resynthesis of acids back into substrate stores (18). Interestingly, gene expression studies on laser-captured motor neurons from patients with ALS showed reduced mRNA levels of α-glucosidase, an enzyme that degrades glycogen to glucose (13). Similar studies on laser-captured astrocytes from $SOD1^{G93A}$ mice also demonstrated more than twofold increases in glycogen synthase mRNA (19).

Therefore, we have now investigated whether $SOD1^{G93A}$ mice undergo metabolic changes favoring development of acidosis and whether they display disease-related pH changes in the CNS. Further, we examined whether the disease course affects the concentration of ions responsible for the SID_{app}, SID_{eff}, and SIG, and whether $SOD1^{G93A}$ mice display compensatory increased glycogen or modifications in α-glucosidase activity to avert acidosis. We also examined human ALS autopsied cervical spinal cord for changes in glycogen content and α-glucosidase activity to determine whether the mouse data are relevant for humans.

Results

Mice Display Progressive CNS Acidosis as ALS Advances. Before determining whether pH changes occur as a function of disease progression in ALS mice, we first measured pH in male wild-type hybrid (B6SJL) mice ($n = 12$). Within the CNS, significant ($P < 0.001$) regional variations in pH were observed with the spinal cord being the most acidic (Fig. 1*A*). To determine whether there were disease-related changes in CNS pH, measurements were made when the mice ($n = 11$ per disease phase) were at symptom onset (SYMP), end stage (ES), and moribund (MB). No significant differences in pH were observed between WT and SYMP $SOD1^{G93A}$ mice (Fig. 1 *B–F*). However, at the ES stage, significantly lower pH values ($P < 0.0001$) were observed in the right

Author contributions: J.C.D. designed research; J.C.D., C.M.T., J.A.F., T.J.T., C.B., M.S., T.V.T., and K.M. performed research; J.C.D., R.L.S., S.H.C., and L.S.S. analyzed data; and J.C.D., R.L.S., S.H.C., and L.S.S. wrote the paper.

The authors declare no conflict of interest.

[1]To whom correspondence may be addressed. E-mail: richard_sidman@hms.harvard.edu or jim.dodge@genzyme.com.

This article contains supporting information online at www.pnas.org/lookup/suppl/doi:10.1073/pnas.1308421110/-/DCSupplemental.

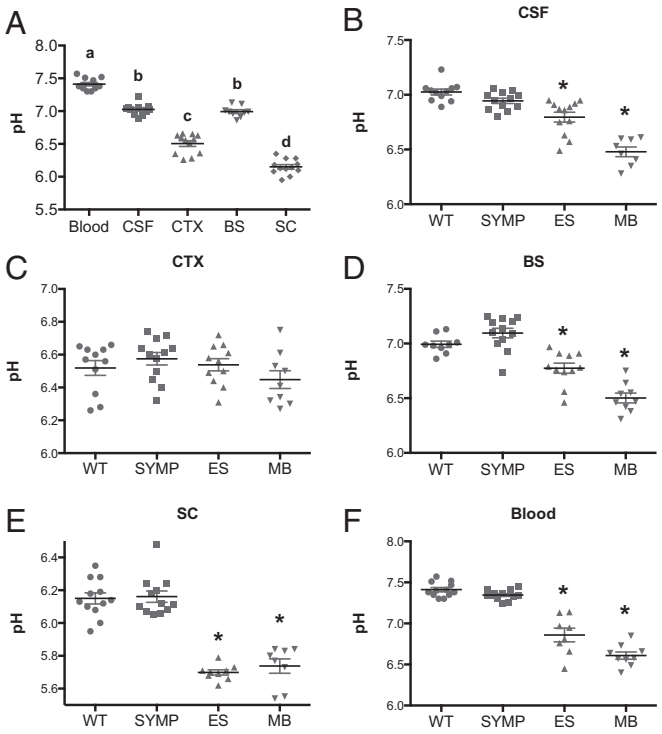

Fig. 1. pH varies significantly as a function of sample matrix (blood, CSF, and CNS parenchyma) and ALS disease course. (*A*) pH measurements in the blood, CSF, motor cortex (CTX), brainstem (BS) (motor trigeminal nucleus), and lumbar spinal cord (SC) of WT mice. Letters not connected by the same letter differ significantly from each other ($P < 0.0001$). pH measurements in ALS mice as a function of disease state vs. WT littermate controls in (*B*) CSF, (*C*) cortex, (*D*) brainstem, (*E*) spinal cord, and (*F*) blood. Significantly different from WT (*$P < 0.0001$). Error bars represent the ±SEM.

lateral ventricle, brainstem, and lumbar spinal cord, as well as in the blood (Fig. 1 *B–E*). No significant differences in pH were observed between WT and ES SOD1^{G93A} within the motor cortex. MB SOD1^{G93A} mice displayed even lower pH values ($P < 0.01$) in the right lateral ventricle, brainstem, and blood, compared with ES SOD1^{G93A} mice (Fig. 1 *B–F*). Measurements in lumbar spinal cord were comparable in ES and MB SOD1^{G93A} mice (Fig. 1*E*). Our data on increasing acidosis within the lumbar spinal cord agree with recent findings in C57BL/6 SOD1^{G93A} mice by an alternative pH measuring method (14). Thus, as the mouse ALS disease advanced, the CNS developed progressively greater acidosis.

Impact of Disease Course in ALS Mice on Major Determinants of H^+ Concentration. Blood samples were collected from male WT and ALS (at SYMP and ES) mice at 10:00 AM and 6:00 PM ($n = 6$ per group per time point) and their serum chemistries (concentration of Na^+, K^+, Mg^{2+}, Ca^{2+}, Cl^-, lactate, CO_2, albumin, and PO_4^{-3} ions) were analyzed (Table S1). Blood from ES mice (i.e., mice that displayed significant declines in CNS pH) had significant reductions in K^+, Mg^{2+}, and Ca^{2+} cations at 10:00 AM ($P < 0.01$) compared with WT mice. No significant changes in cation levels were observed in ALS mice at 6:00 PM except for Ca^{2+}, which was significantly lower ($P < 0.01$) in both SYMP and ES mice. The concentrations of Cl^- and lactate anions were also impacted during the course of the disease, with significant reductions ($P < 0.01$) in both Cl^- and lactate levels. Reductions in Cl^- were limited to SYMP mice at 6:00 PM, whereas reductions in lactate were observed in both SYMP and ES mice at 10:00 AM. Blood levels of CO_2, PO_4^{-3} and albumin (ions used to calculate the SID_{eff}) in ALS mice at 10:00 AM were not affected during the disease course. However, significant reductions in albumin ($P < 0.01$) were observed in SYMP and ES mice at 6:00 PM. Alterations in serum ion levels are limited (in some cases) to specific circadian time points in ALS mice for reasons that are not well understood, perhaps attributable to various factors including potential disease-related differences in metabolic activity at the sampled time points (e.g., 10:00 AM = postprandial per rest phase; 6:00 PM = preprandial per onset of activity phase).

Ion concentrations were then used to calculate SID_{app}, SID_{eff}, and SIG in serum by the equations given in the Introduction. In the first reported measurements in mice, we found that WT mice display a SID_{app} value of 43.02 ± 1.73, and similar values were found in SYMP (44.26 ± 1.65) and ES (41.60 ± 1.70) ALS mice (Fig. 2*A*), consistent with previous measurements in normal mammals (13). Interestingly, calculations of SID_{eff}, which takes into account the additional contribution of weak acids, showed significant ($P < 0.01$) differences between WT and ES mice (46.46 ± 1.85 vs. 30.03 ± 1.87; Fig. 2*A*). The SIG was then calculated by subtracting SID_{eff} from SID_{app}. A SIG value greater than zero indicates presence of unexplained anions, whereas a SIG of less than zero suggests presence of unexplained cations. We found that ES mice displayed a positive SIG value compared with their WT counterparts (11.57 ± 0.22 vs. −3.44 ± 0.16; Fig. 2*A*). Hence, careful examination of pH and SIG may represent a unique approach to track disease progression in patients with ALS.

Carbonic Anhydrase Inhibition Accelerates Mouse ALS. Carbonic anhydrase catalyzes the conversion of CO_2 and H_2O to HCO_3^- and its inhibition leads to elevated CO_2 levels (acidosis). Cats and rabbits given acetazolamide (a carbonic anhydrase inhibitor) show significant reductions in pH within the brain (20, 21). Therefore, we examined the impact of acetazolamide on ALS mice. ALS mice ($n = 10$) administered acetazolamide (beginning on day 60) displayed a more rapid decline in hindlimb grip strength ($P < 0.01$), an earlier onset of paralysis (114 vs. 120 d; $P < 0.01$), and a trend toward accelerated death (122 vs. 134.5 d) vs. control siblings treated with vehicle (Fig. 2 *B–D*). Grip strength (Fig. 2*B*) and lifespan were unaffected in WT mice treated with acetazolamide. These findings indicate that promotion of acidosis in ALS mice accelerates disease progression. Furthermore, prescribing carbonic anhydrase inhibitors to treat hypertension,

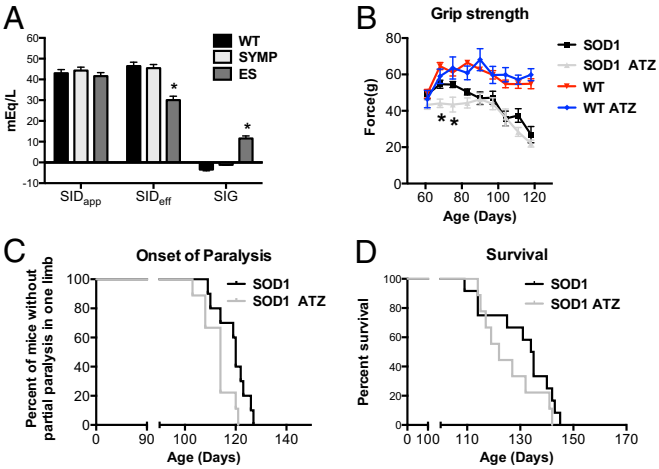

Fig. 2. Impact of ALS on the major determinants of [H^+] and the rate of disease progression in ALS mice following administration of acetazolamide (pH lowering agent). (*A*) Calculated apparent strong ion difference (SID_{app}), effective strong ion difference (SID_{eff}), and strong ion gap (SIG) in ALS mice as function of disease state vs. WT littermate controls. (*B*) Hindlimb grip strength, (*C*) median end stage (partial paralysis in one limb) age, and (*D*) median survival age following daily treatment with acetazolamide (ATZ, ~30 mg/kg). Significantly different from WT (*$P < 0.01$). Error bars represent ±SEM.

glaucoma, or migraine headaches in patients with ALS may be contraindicated.

ALS Mice Display Aberrant Glycogen Increases in CNS and Viscera. Pathological acidosis is typically averted by decreasing acid synthesis and/or enhancing acid elimination (18). Therefore, we determined whether ALS mice harbored changes in glucose and glycogen levels interpretable as responses counteracting pathological acidosis. Glucose levels in the CNS of WT mice ($n = 6$) showed significant regional variation ($P < 0.0001$), with levels in cerebral cortex (CTX) > midbrain (MB) > cerebellum (CB) = brainstem (BS) > lumbar spinal cord (SC) (Fig. 3*A*). Similar regional variations in glucose levels were observed in the CNS of ALS mice ($n = 6$ per disease phase) (Fig. 3*A*). In contrast, glycogen levels were comparable throughout the CNS of WT and ALS mice (Fig. 3*A*). In cerebral cortex, although the glucose levels in ALS mice were lower ($P < 0.05$), the glycogen levels in WT and ALS mice were similar (Fig. 3*A*), as they were in midbrain and cerebellum. However, in brainstem and lumbar spinal cord, ALS mice displayed significantly higher levels of glycogen compared with WT ($P < 0.0001$) (Fig. 3*A*). Notably, the timing of abnormal glycogen accumulation in the CNS of ALS mice was coincident with significant declines in pH (shown above). Indeed, linear regression analysis showed that disease-related changes in pH and glycogen were significantly ($P < 0.004$) correlated ($r^2 = 0.7714$, Fig. S1).

As increased excretion of acids from the CNS into the periphery might occur (protecting the CNS from aberrant carbohydrate metabolism), we also measured glucose and glycogen levels in liver, muscle, and kidney of ALS mice at two circadian times (10:00 AM and 6:00 PM; $n = 6$ per disease phase per time point). In liver and muscle, circadian variations in glucose and glycogen were observed, with carbohydrate levels higher at 10:00 AM than at 6:00 PM (Fig. 4 *A* and *B*). Glucose levels in liver were comparable between ALS and WT mice at all sampled time points; however, glycogen levels were four- to fivefold higher in ALS mice at 10:00 AM ($P < 0.001$) (Fig. 4*A*). Interestingly, increased glycogen was observed in SYMP mice, which was before detection of disease-related changes in pH. In muscle, significant reductions in glucose and concomitant elevations in glycogen were also observed in SYMP and ES mice. At 6:00 PM, glucose levels were significantly lower ($P < 0.05$) and glycogen levels higher ($P < 0.05$) in both SYMP and ES mice than in their WT counterparts (Fig. 4*B*). In kidney, significantly ($P < 0.01$) higher levels of glucose and significantly ($P < 0.01$) lower levels of glycogen were detected in ALS mice, perhaps reflecting that more glucose and lactate were excreted into urine with less being stored as glycogen (Fig. 4*C*). Collectively, our findings showed that changes in glucose and glycogen levels occurred in peripheral tissues before any overt signs of disease.

Patients with ALS Harbor Increased Glycogen in the Spinal Cord. To determine whether carbohydrate levels are also modified in humans with ALS, we examined cervical spinal tissue samples collected at autopsy from male patients with ALS ($n = 6$) and aged matched male controls ($n = 6$). For patient donor information please see *Supporting Information* (Table S2). Glucose levels were significantly ($P < 0.01$) elevated in tissue homogenates of gray matter (GM) from ALS vs. control individuals (Fig. 3*B*), although levels in ventral white matter (VWM) homogenates were comparable in ALS and control samples. Similar to what was observed in $SOD1^{G93A}$ mice, glycogen levels were significantly elevated in both GM ($P < 0.01$) and VWM ($P < 0.001$) ALS vs. control tissue homogenates (Fig. 3*B*). To determine which cell types harbored increased glycogen, periodic acid-Schiff (PAS) staining on paraffin-embedded cervical spinal cord sections showed increased glycogen in residual GM neurons and glia (Fig. 3*C*) and in VWM glia (Fig. 3*D*). Consistent with our biochemical findings, PAS staining appeared to be both stronger and more widespread in ALS vs. control

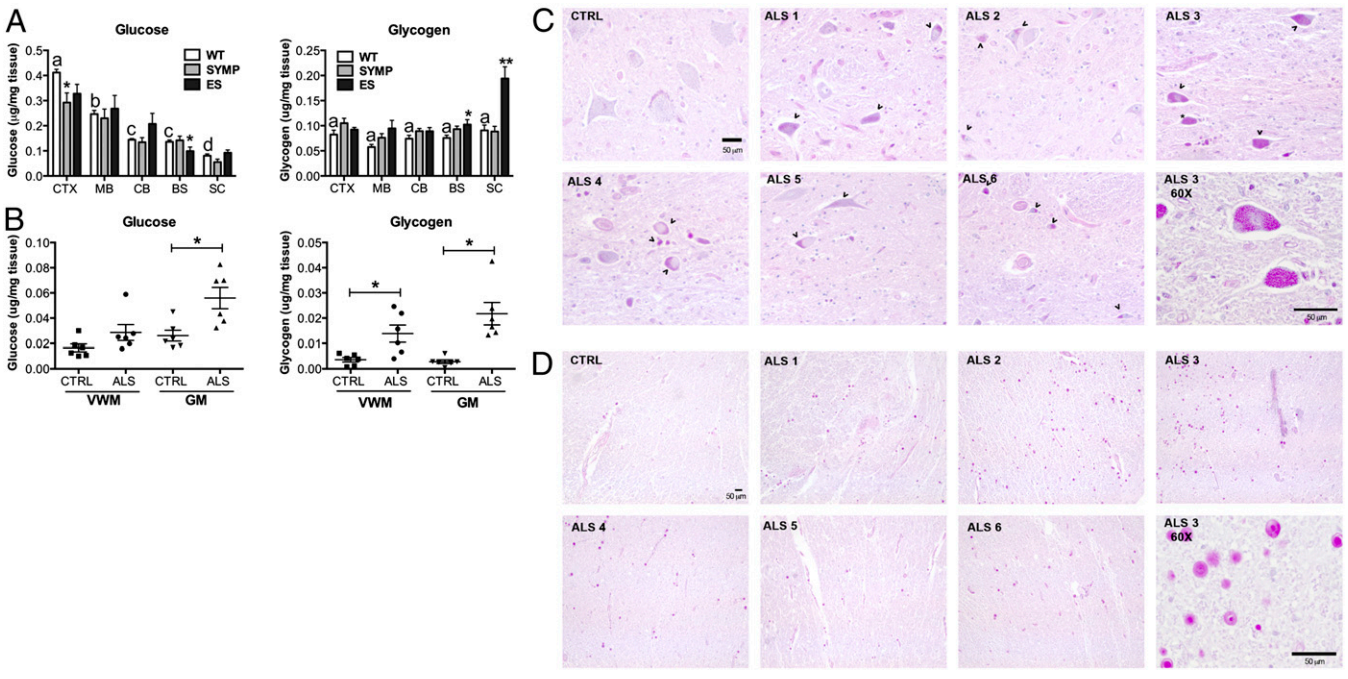

Fig. 3. Tissue levels of glucose and glycogen are affected by ALS disease course in mice and humans. (*A*) Glucose and glycogen levels as a function of CNS region (CTX, cerebral cortex; MB, midbrain; CB, cerebellum; BS, brainstem; and SC, lumbar spinal cord) in ALS mice as function of disease (SYMP, symptomatic stage; and ES, end stage vs. WT littermate controls. Significantly different from WT (*$P < 0.05$, **$P < 0.0001$). Bars with different letter are significantly different from each other ($P < 0.0001$). (*B*) Glucose and glycogen levels in human ALS and control (CTRL) cervical spinal cord tissue homogenates (GM, gray matter; VWM, ventral white matter). Significantly different from CTRL (*$P < 0.001$). Error bars represent ±SEM. (*C* and *D*) Paraffin-embedded, PAS-stained cervical spinal sections of human ALS and CTRL donors (*C*, GM; *D*, VWM; arrowheads point to glycogen storage; all images are at 20× cells except for panels at 60× in the *Lower Right* corner in *C* and *D*. (Scale bars, 50 μm.)

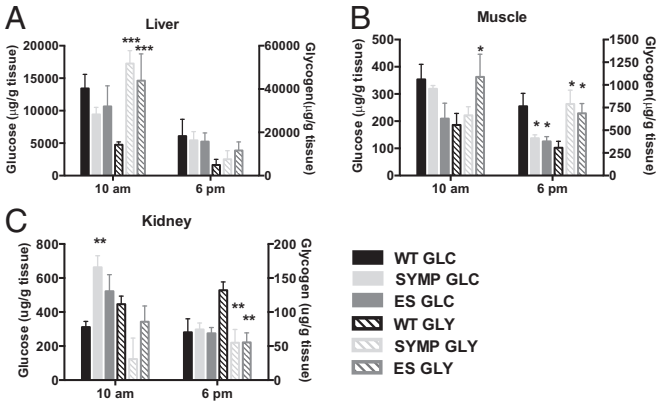

Fig. 4. Glucose (GLC) and glycogen (GLY) levels in peripheral tissues are affected by ALS disease course. GLC and GLY levels measured in (*A*) liver, (*B*) muscle, and (*C*) kidney of ALS mice as a function of disease phase vs. WT littermate controls at two circadian times (SYMP, symptomatic; ES, end stage). Significantly different from WT (*$P < 0.05$, **$P < 0.01$, ***$P < 0.001$). Error bars represent ±SEM.

tissue (Fig. 3 *C* and *D*). Collectively, these findings suggest that glycogen accumulation in spinal cord is a common feature of ALS.

ALS Mice Show Changes in α-Glucosidase Activity. Reduced α-glucosidase mRNA levels have been reported in laser-captured motor neurons from spinal cords of patients with ALS (13). Deficiency in lysosomal acid α-glucosidase activity leads to Pompe disease, a "neuromuscular" lysosomal storage disease characterized by aberrant glycogen accumulation in both viscera and CNS (22, 23). Neutral (endoplasmic reticulum, ER) α-glucosidase trims glucose residues from N-glycans of glycoproteins, which is part of an elaborate and important quality-control system that promotes the proper folding and oligomerization of newly formed proteins and their transport from the ER to their final destination (24). We examined acidic and neutral α-glucosidase enzyme activities in spinal cord, muscle, liver, and serum as a function of disease progression in ALS ($n = 5$ per disease phase) vs. WT ($n = 5$) mice. All samples were collected at 10:00 AM. No significant changes in enzyme activity were observed between WT and ALS mice in serum, but in spinal cord, a significant ($P < 0.01$) reduction in acid α-glucosidase activity was found in SYMP and ES vs. WT mice (Fig. 5*A*). In contrast, neutral enzyme activity was significantly ($P < 0.001$) elevated more than twofold in ES (i.e., in mice, at the onset of paralysis) vs. WT counterparts (Fig. 5*A*). In muscle and liver, both acidic and neutral α-glucosidase activities were significantly ($P < 0.001$) elevated two- to eightfold (Fig. 5 *B* and *C*) in ES mice vs. WT counterparts. Interestingly, enzyme activity levels varied across different tissues, and were significantly greater in liver ($P < 0.001$) and muscle ($P < 0.01$) than in spinal cord (Fig. 5*D*).

Neutral α-Glucosidase Activity Is Elevated in Patients with ALS. Our findings of altered α-glucosidase enzyme activity in SOD1^{G93A} mice prompted us to examine acidic and neutral enzyme activities in GM and VWM tissue homogenates from male patients with ALS ($n = 6$) vs. age-matched male controls ($n = 6$). In contrast to our findings in ALS mice, we observed a trend toward an elevation in acidic α-glucosidase activity (Fig. 5 *E* and *F*), suggesting that a reduction in acidic α-glucosidase activity may be limited to the SOD1^{G93A} model. Alternatively, disease-related changes in enzyme activity might be species specific. However, consistent with our observations in SOD1^{G93A} mice, a significant elevation in neutral α-glucosidase activity was noted in human ALS cervical spinal cord GM samples (Fig. 5*E*), and not in the VWM (Fig. 5*F*). Importantly, linear regression analysis showed that glucose levels in spinal cord GM correlated significantly ($P < 0.001$) with neutral ($r^2 = 0.6477$) and acidic ($r^2 = 0.6147$) glucosidase enzyme activity. In VWM, a significant ($P < 0.001$) correlation was also observed between glycogen levels and neutral ($r^2 = 0.4142$) and acidic ($r^2 = 0.8172$) glucosidase activities (Fig. S2). Recently developed human cell culture models of ALS (25) could be used to further elucidate the relationship between glucose, glycogen, and glucosidase enzyme activity within specific cell types in gray and white matter.

Discussion

We show here that the SOD1^{G93A} mouse model of ALS enters a state of progressive acidosis associated with manifold metabolic alterations present also in autopsied human ALS spinal cord samples. Several lines of evidence indicate that acidosis is not merely a consequence of disease, but is a significant modulator of disease progression. For example, in a controlled clinical trial, the intake of branched chain amino acids (exogenous acids) led to accelerated loss of pulmonary function in patients with ALS (26). Also, a faster rate of decline in muscle strength was observed in patients with ALS treated with Topiramate (Apotex Corp.), a known inhibitor of carbonic anhydrase (a crucial enzyme that buffers pH and helps maintain acid-base balance) (27). Consistent with these observations, we showed that motor functional decline and onset of paralysis were accelerated in ALS mice upon administration of acetazolamide, another carbonic anhydrase inhibitor. The carbonic acid (H_2CO_3)–bicarbonate (HCO_3^-) system ($CO_2 + H_20 \leftrightarrow H_2CO_3 \leftrightarrow H^+ + HCO_3^-$) is central to maintaining acid-base balance through its ability to provide rapid adjustments to changing levels of volatile [partial carbon dioxide tension (pCO_2)] and nonvolatile acids (hydrochloric, sulfuric, lactic, etc.).

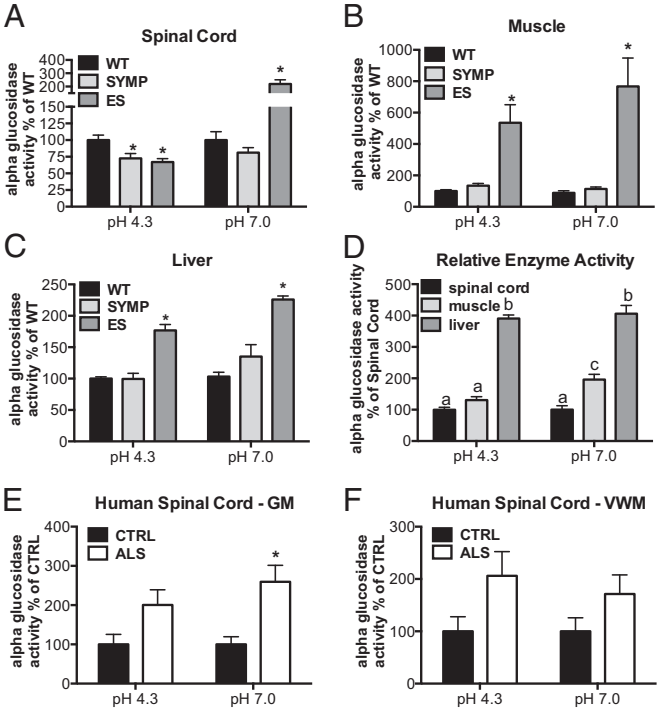

Fig. 5. α-Glucosidase activity is affected by ALS disease course in mice and patients. Lysosomal (pH 4.3) and neutral (pH 7.0) α-glucosidase activities were measured in ALS mice as a function of disease phase vs. WT littermate controls (SYMP, symptomatic; ES, end stage) in (*A*) spinal cord, (*B*) muscle, and (*C*) liver. Significantly different from WT (*$P < 0.001$). (*D*) Relative enzyme activity across different tissues (in WT mice) graphed relative to spinal cord levels. Bars with different letters are significantly different from each other ($P < 0.01$). (*E* and *F*) Lysosomal (acidic) and neutral α-glucosidase activities in human ALS and control (CTRL) cervical spinal cord tissue homogenates (GM, gray matter; VWM, ventral white matter). Significantly different from CTRL (*$P < 0.01$). Error bars represent ±SEM.

The relationship between volatile (i.e., respiratory) and nonvolatile (i.e., metabolic) acids is best understood through an extension of the Henderson–Hasselbalch equation ($pH = pK \times \log [HCO_3^-/(0.03 \times pCO_2)]$) (28). Either an increase in pCO_2 or a drop in $[HCO_3^-]$ will trigger a decrease in pH. Hyperventilation is a compensatory response initiated by nonvolatile acid accumulation, because it decreases pCO_2, which in turn promotes the dissociation of H_2CO_3 into CO_2 and H_20. As H_2CO_3 dissociates (and CO_2 is expelled by the lungs) H^+ removal (alkalization) is promoted as H^+ combines with HCO_3^-. Given these processes, it is not surprising that an increase in breathing frequency, tidal volume, and CO_2 production was found to occur in $SOD1^{G93A}$ mice several weeks before death (29). Sustained hyperventilation leading to CO_2 depletion within the CNS, however, will initiate vasoconstriction, reduced blood flow, ischemia, and edema (30)—all occurring in the spinal cord of $SOD1^{G93A}$ mice before motor neuron degeneration (31, 32).

Pathological acidosis in ALS could be attributed to a number of events arising as the disease progresses. These include metabolic abnormalities, increased muscle catabolism, impaired respiratory function (although the latter does not occur until a few days before death in $SOD1^{G93A}$ mice (29), whereas we observed acidosis ∼20 d before death) and the accumulation of an as yet undetermined anion. Indeed, we showed that $SOD1^{G93A}$ mice present several changes indicative of altered lipid metabolism (e.g., reduced circulating triglyceride levels, reduced fat mass, increased circulating levels of the lipolytic hormone glucagon, and decreased levels of the antilipolytic hormone insulin), which, when prolonged, can trigger acidosis (Fig. S3). Interestingly, the changes in glucagon and insulin preceded reductions in fat mass and the development of pathological acidosis. We also recently reported that $SOD1^{G93A}$ mice displayed pathological elevations in the lipolytic hormone, corticosterone, which significantly correlated with accelerated disease progression (33). The reason why increases in lipid metabolism manifest during ALS remains unclear. During ALS progression the CNS may become more dependent on alternative fuels (lipids, ketones, amino acids) to generate energy when glucose flux through the glycolytic pathway is diminished (34). Our finding of an increased SIG also suggests that an unknown anion may be responsible, in part, for the development of acidosis in ALS mice. We showed that at the ES stage, the SIG value approaches 12 mEq/L, which is particularly interesting given that SIG values greater than 10 are reportedly the strongest predictor of mortality in individuals exposed to pathological acidosis (16).

A variety of compensatory mechanisms that either lower acid production, promote acid elimination, or both may help to avert pathological acidosis (18). Glucose utilization (35) and monocarboxylate transporter 1 (MCT1)-mediated lactate uptake (36) within the CNS are inhibited by acidosis. Indeed, glucose uptake and/or levels within the CNS are significantly diminished in patients with ALS (37), $SOD1^{G93A}$ mice (32, 38), and in WT mice exposed to cerebrospinal fluid (CSF) from patients with ALS (39). Moreover, lactate levels are reduced in spinal cords of $SOD1^{G93A}$ mice (19), as is the expression of MCT1 (36). Our results extend these findings. Concomitant with the reductions in pH, significant accumulation of glycogen was observed in both the CNS and visceral organs of $SOD1^{G93A}$ mice. Within the ALS mouse CNS, reductions in pH were highly correlated ($r^2 = 0.7714$) with glycogen accumulation. Importantly, spinal cord glycogen accumulation also appears to be a prominent feature of human ALS. Specifically, we found elevated glycogen in gray and ventral white matter samples from autopsied patients with ALS, confirmed by histological analyses showing elevated glycogen in both neurons and glia. The increased glycogen in the CNS of $SOD1^{G93A}$ mice and humans with ALS is consistent with spinal cord gene expression profiling studies from ALS mice and humans that showed elevated glycogen synthase mRNA levels and altered α-glucosidase mRNA (13, 19). Indeed, we show here that lysosomal (glycogen degrading) α-glucosidase activity is significantly reduced within the lumbar spinal cord of $SOD1^{G93A}$ mice in advance of the onset of hindlimb paralysis. However, lower acidic α-glucosidase activity was not observed in the spinal cord samples from patients with ALS, so this feature may be limited to mutant SOD1-related ALS. Nevertheless, therapeutic possibilities are suggested, given that rapamycin, a drug recently reported to lower glycogen levels in α-glucosidase knockout mice (40) (a model of Pompe disease) was also shown to accelerate disease in $SOD1^{G93A}$ mice (41). Accelerated disease progression in ALS mice following treatment that reduces glycogen levels is consistent with the data indicating that glycogen increase slows the disease course.

We also measured the activity of neutral α-glucosidase, an ER resident enzyme that plays a critical role in the processing of N-glycans attached to glycoproteins to ensure proper folding. Removal of glucose residues by neutral α-glucosidase generates a monoglycosylated epitope that is recognized by lectin chaperones (i.e., calnexin and calreticulin) to maintain the protein within the ER until proper folding is achieved. Removal of the last glucose residue leads to the misfolded protein being transported to the proteasome for degradation (24). Enzyme activity was elevated more than twofold in the spinal cords of ES mice, as well as being significantly elevated in spinal cords of patients with ALS. We speculate that the continuous trimming of glucose residues from misfolded proteins by neutral α-glucosidase (to promote protein refolding) may also contribute to aberrant glucose homeostasis (and potentially to glucose neurotoxicity) (42) within the spinal cord. Indeed, our measured significant glucose accumulation within spinal cords of patients with ALS significantly correlated ($r^2 = 0.6477$) with α-glucosidase enzyme activity.

Changes in glycogen content were also observed in peripheral tissues of ALS mice, perhaps due in part to glucose and/or lactate export from the CNS, serving to protect the CNS from pathological acidosis and neurotoxicity. We were surprised to find elevated acidic (lysosomal) α-glucosidase activity in peripheral tissues and speculate that lysosomal α-glucosidase activity may increase in peripheral tissues when glycogen levels in the CNS become pathogenic, at which point glycogen must be metabolized to glucose and excreted. In agreement with this hypothesis, we observed that $SOD1^{G93A}$ mice had significantly increased glucose levels in kidneys (despite normal serum levels) and had 2.2–8.6-fold increases in α-glucosidase activities in liver and muscle of ES vs. WT mice. We noted also that basal neutral α-glucosidase activity in WT mice is 1.7- and 4-fold greater in muscle and liver, respectively, vs. spinal cord. Both the basal- and disease-induced differences in neutral α-glucosidase activity within muscle and liver may explain in part why misfolded SOD1 protein was detected at significantly higher levels in CNS than in peripheral tissues in mouse ALS (43, 44). Our point of emphasis is that this mouse ALS model displays significant glycogen increases in both CNS and peripheral tissues.

Developing drugs to alleviate acidosis and slow progression of ALS will be challenging. Although we also found significant upregulation of ASIC mRNA in the spinal cords of $SOD1^{G93A}$ ALS mice, treatment with amiloride, an ASIC blocker that can lessen disease severity in rodent models of multiple sclerosis, Parkinson disease, and ischemia (diseases also featuring acidosis) (5–7), failed to slow disease progression in the ALS mice model (Fig. S4). This may reflect the fact that several neuropathological features catalyzed by acidosis also occur independently of ASIC activation. Given our current findings, it is also no surprise that assisted ventilation (e.g., with bilevel positive airway pressure, BiPAP) has been linked to extended survival rates in patients with ALS (45, 46). Clearly, assisted ventilation would be most helpful during periods of acidosis.

In summary, our data showed that $SOD1^{G93A}$ mice and humans with ALS share several metabolic abnormalities indicative of increased lipolysis and pathological acidosis. The disease also affected serum concentrations of ions used to calculate the SID_{app}, SID_{eff}, and SIG, strongly suggesting that development of pathological acidosis was likely due in part to the presence of an unidentified anion. Furthermore, $SOD1^{G93A}$ mice display metabolic changes indicative of a compensatory response that may help

avert pathological acidosis. Our results also demonstrated that glycogen increase and fluctuations in α-glucosidase activity in the spinal cord are robust features of human ALS. Collectively, our work provides fresh insight into the pathogenesis of ALS as well as potential biomarkers and targets for drug development.

Materials and Methods

Transgenic male ALS mice that strongly express the mutant SOD1^{G93A} transgene were divided into equivalent groups. Mutant SOD1^{G93A} gene copy number and protein expression were confirmed by PCR and Western blot analysis, respectively. Animals were housed under light:dark (12:12 h) cycles and provided with food and water ad libitum. At 75 d of age, food pellets were place on the cage floor to facilitate access to food by weakening mice. Mice were scored as symptomatic (SYMP), showing abnormal hindlimb splay, median age 82 d; end stage (ES), with onset of limb paralysis (typically hindlimb), median age 103 d; and moribund (MB), unable to right themselves within 30 s after being placed on their backs, median age 122 d. All procedures were performed using protocols approved by Genzyme's Institutional Animal Care and Use Committees. Please see *SI Materials and Methods* for further details.

ACKNOWLEDGMENTS. Human tissue was obtained from the National Institute of Child Health and Human Development Brain and Tissue Bank for Developmental Disorders at the University of Maryland, Baltimore, Contact HHSN275200900011C, Ref. N01-HD-9-0011.

1. Rosen DR (1993) Mutations in Cu/Zn superoxide dismutase gene are associated with familial amyotrophic lateral sclerosis. *Nature* 364(6435):362.
2. Gurney ME, et al. (1994) Motor neuron degeneration in mice that express a human Cu,Zn superoxide dismutase mutation. *Science* 264(5166):1772–1775.
3. Bruijn LI, Miller TM, Cleveland DW (2004) Unraveling the mechanisms involved in motor neuron degeneration in ALS. *Annu Rev Neurosci* 27:723–749.
4. Teng YD, et al. (2012) Multimodal actions of neural stem cells in a mouse model of ALS: A meta-analysis. *Science Transl Med* 4(165):165ra164.
5. Ames A, 3rd, Maynard KI, Kaplan S (1995) Protection against CNS ischemia by temporary interruption of function-related processes of neurons. *J Cereb Blood Flow Metab* 15(3): 433–439.
6. Arias RL, et al. (2008) Amiloride is neuroprotective in an MPTP model of Parkinson's disease. *Neurobiol Dis* 31(3):334–341.
7. Friese MA, et al. (2007) Acid-sensing ion channel-1 contributes to axonal degeneration in autoimmune inflammation of the central nervous system. *Nat Med* 13(12):1483–1489.
8. Swanson RA, Farrell K, Simon RP (1995) Acidosis causes failure of astrocyte glutamate uptake during hypoxia. *J Cereb Blood Flow Metab* 15(3):417–424.
9. Khan NA, Guevara P, Sotelo J (1989) Influence of in vitro lactic acidosis on central nervous system neurons. *Pathol Biol (Paris)* 37(6):725–729.
10. Morihata H, Nakamura F, Tsutada T, Kuno M (2000) Potentiation of a voltage-gated proton current in acidosis-induced swelling of rat microglia. *J Neurosci* 20(19):7220–7227.
11. Aoyama K, et al. (2005) Acidosis causes endoplasmic reticulum stress and caspase-12-mediated astrocyte death. *J Cereb Blood Flow Metab* 25(3):358–370.
12. Erecińska M, Nelson D, Dagani F, Deas J, Silver IA (1993) Relations between intracellular ions and energy metabolism under acidotic conditions: A study with nigericin in synaptosomes, neurons, and C6 glioma cells. *J Neurochem* 61(4):1356–1368.
13. Kirby J, et al. (2011) Phosphatase and tensin homologue/protein kinase B pathway linked to motor neuron survival in human superoxide dismutase 1-related amyotrophic lateral sclerosis. *Brain* 134(Pt 2):506–517.
14. Behan AT, et al. (2013) Acidotoxicity and acid-sensing ion channels contribute to motoneuron degeneration. *Cell Death Differ* 20(4):589–598.
15. Rinaldi S, De Gaudio AR (2005) Strong ion difference and strong anion gap: The Stewart approach to acid base disturbances. *Curr Anaesth Crit Care* 16(6):395–402.
16. Kaplan LJ, Kellum JA (2004) Initial pH, base deficit, lactate, anion gap, strong ion difference, and strong ion gap predict outcome from major vascular injury. *Crit Care Med* 32(5):1120–1124.
17. Kaplan LJ, Kellum JA (2010) Fluids, pH, ions and electrolytes. *Curr Opin Crit Care* 16(4): 323–331.
18. Sestoft L, Bartels PD (1983) Biochemistry and differential diagnosis of metabolic acidoses. *Clin Endocrinol Metab* 12(2):287–302.
19. Ferraiuolo L, et al. (2011) Dysregulation of astrocyte-motoneuron cross-talk in mutant superoxide dismutase 1-related amyotrophic lateral sclerosis. *Brain* 134(Pt 9):2627–2641.
20. Bickler PE, Litt L, Banville DL, Severinghaus JW (1988) Effects of acetazolamide on cerebral acid-base balance. *J Appl Physiol* 65(1):422–427.
21. Heuser D, Astrup J, Lassen NA, Betz BE (1975) Brain carbonic acid acidosis after acetazolamide. *Acta Physiol Scand* 93(3):385–390.
22. Hirshhorn R, Reuser AJJ (2001) Glycogen storage disease type II: Acid alpha-glucosidase (acid maltase) deficiency. *The Metabolic and Molecular Bases of Inherited Disease*, eds Scriver CA, Beaudet AL, Valle D, Sly WS (McGraw–Hill, New York), 8th Ed, pp 3389–3420.
23. Sidman RL, et al. (2008) Temporal neuropathologic and behavioral phenotype of 6neo/6neo Pompe disease mice. *J Neuropathol Exp Neurol* 67(8):803–818.
24. Herscovics A (1999) Importance of glycosidases in mammalian glycoprotein biosynthesis. *Biochim Biophys Acta* 1473(1):96–107.
25. Haidet-Phillips AM, et al. (2011) Astrocytes from familial and sporadic ALS patients are toxic to motor neurons. *Nat Biotechnol* 29(9):824–828.
26. Tandan R, et al. (1996) A controlled trial of amino acid therapy in amyotrophic lateral sclerosis: I. Clinical, functional, and maximum isometric torque data. *Neurology* 47(5): 1220–1226.
27. Cudkowicz ME, et al.; Northeast ALS Consortium (2003) A randomized, placebo-controlled trial of topiramate in amyotrophic lateral sclerosis. *Neurology* 61(4):456–464.
28. Chesler M (1990) The regulation and modulation of pH in the nervous system. *Prog Neurobiol* 34(5):401–427.
29. Tankersley CG, Haenggeli C, Rothstein JD (2007) Respiratory impairment in a mouse model of amyotrophic lateral sclerosis. *J Appl Physiol* 102(3):926–932.
30. Ainslie PN, Duffin J (2009) Integration of cerebrovascular CO2 reactivity and chemoreflex control of breathing: Mechanisms of regulation, measurement, and interpretation. *Am J Physiol Regul Integr Comp Physiol* 296(5):R1473–R1495.
31. Zhong Z, et al. (2008) ALS-causing SOD1 mutants generate vascular changes prior to motor neuron degeneration. *Nat Neurosci* 11(4):420–422.
32. Miyazaki K, et al. (2012) Early and progressive impairment of spinal blood flow-glucose metabolism coupling in motor neuron degeneration of ALS model mice. *J Cereb Blood Flow Metab* 32(3):456–467.
33. Fidler JA, et al. (2011) Disease progression in a mouse model of amyotrophic lateral sclerosis: The influence of chronic stress and corticosterone. *FASEB J* 25(12):4369–4377.
34. Chang Y, et al. (2008) Messenger RNA oxidation occurs early in disease pathogenesis and promotes motor neuron degeneration in ALS. *PLoS ONE* 3(8):e2849.
35. Newman GC, Hospod FE, Schissel SL (1991) Ischemic brain slice glucose utilization: Effects of slice thickness, acidosis, and K+. *J Cereb Blood Flow Metab* 11(3):398–406.
36. Uhernik AL, Tucker C, Smith JP (2011) Control of MCT1 function in cerebrovascular endothelial cells by intracellular pH. *Brain Res* 1376:10–22.
37. Dalakas MC, Hatazawa J, Brooks RA, Di Chiro G (1987) Lowered cerebral glucose utilization in amyotrophic lateral sclerosis. *Ann Neurol* 22(5):580–586.
38. Browne SE, et al. (2006) Bioenergetic abnormalities in discrete cerebral motor pathways presage spinal cord pathology in the G93A SOD1 mouse model of ALS. *Neurobiol Dis* 22(3):599–610.
39. Godoy JM, Skacel M, Lima JM, Andrade CM (1990) *Arqu Neuro-Psiqu* 48(4):473–477.
40. Ashe KM, et al. (2010) Inhibition of glycogen biosynthesis via mTORC1 suppression as an adjunct therapy for Pompe disease. *Mol Genet Metab* 100(4):309–315.
41. Zhang X, et al. (2011) Rapamycin treatment augments motor neuron degeneration in SOD1(G93A) mouse model of amyotrophic lateral sclerosis. *Autophagy* 7(4):412–425.
42. Tomlinson DR, Gardiner NJ (2008) Glucose neurotoxicity. *Nat Rev Neurosci* 9(1): 36–45.
43. Rakhit R, et al. (2007) An immunological epitope selective for pathological monomer-misfolded SOD1 in ALS. *Nat Med* 13(6):754–759.
44. Zetterström P, et al. (2007) Soluble misfolded subfractions of mutant superoxide dismutase-1s are enriched in spinal cords throughout life in murine ALS models. *Proc Natl Acad Sci USA* 104(35):14157–14162.
45. Bach JR (1995) Amyotrophic lateral sclerosis: Predictors for prolongation of life by noninvasive respiratory aids. *Arch Phys Med Rehabil* 76(9):828–832.
46. Sancho J, Servera E, Bañuls P, Marín J (2010) Prolonging survival in amyotrophic lateral sclerosis: Efficacy of noninvasive ventilation and uncuffed tracheostomy tubes. *Am J Phys Med Rehabil* 89(5):407–411.